

# A retrospective on the 2025 Atlantic hurricane season

C. W. Powell<sup>1</sup>

<sup>1</sup>ICCS & DAMTP, University of Cambridge, Cambridge, UK

arXiv:2511.23458v2 [physics.ao-ph] 23 Feb 2026

---

Corresponding author: Charles Powell, [cwp29@cam.ac.uk](mailto:cwp29@cam.ac.uk)

**Abstract**

The 2025 Atlantic hurricane season was intermittent, with extended quiet periods separated by three clusters of activity. The broad-scale conditions were often unfavourable for cyclogenesis and common drivers of activity such as La Niña were weak, but well above-average sea temperatures still supported intense storms. Activity was limited by periods of strong vertical shear and a disrupted West African Monsoon, including a lull during the climatological peak of activity in August. During September and October, strong seed disturbances underwent cyclogenesis in the tropical Atlantic, coinciding with Kelvin wave activity and favourable MJO conditions.

**Key points**

1. The 2025 Atlantic hurricane season was marked by extended inactive periods despite warm sea-surface temperatures and a weak La Niña.
2. Cyclogenesis was limited by suppressed African easterly wave amplitudes, dry and stable air, and strong vertical shear driven by a persistent upper-level trough.
3. Kelvin waves and the MJO modulated AEW development during active periods that featured a small number of intense storms.

**1 Introduction**

Tropical cyclone (TC) activity is strongly controlled by sea surface temperatures (SSTs); temperatures exceeding  $26.5^{\circ}\text{C}$  are needed for TC formation (e.g. McTaggart-Cowan et al. (2015)). However, other environmental conditions are required to support the formation of tropical depressions (cyclogenesis), their organisation into coherent deep circulations, and intensification to reach tropical storm strength (Rajasree et al., 2023; McTaggart-Cowan et al., 2015). Factors promoting the formation of TCs include upper-level divergence, which promotes surface convergence (Gray, 1968) and aids the development of ‘seed disturbances’ from which most TCs grow (Sears & Velden, 2014). Cyclogenesis is also favoured by factors that promote deep convection such as large-scale instability and requires the formation of a large column of nearly-saturated air (i.e. large relative humidity (RH), particularly at mid-levels) that allows disturbances to grow efficiently (Emanuel, 2003). Other factors can inhibit TC formation, such as vertical wind shear, which disrupts the organisation of tropical depressions by displacing the low- and upper-level circulation centres and promotes ventilation of dry air into developing TCs (Rios-Berrios, Finocchio, et al., 2024). Similarly, developing convective systems are suppressed in regions with dry mid-level air and large-scale subsidence that increases stability and disrupts low-level convergence. TC activity is therefore influenced by variability in the aforementioned factors.

In the North Atlantic basin, the largest source of interannual variability in TC activity is the El-Niño Southern Oscillation (ENSO). El Niño conditions increase vertical wind shear and subsidence in the Atlantic basin, suppressing TC activity, whilst La Niña conditions tend to favour active seasons via a weakening of upper-level winds (Gray, 1984; Klotzbach, 2011). Whilst some TCs form in-situ, particularly early and late in the season in the Gulf of Mexico and Caribbean Sea (Corporal-Lodangco et al., 2014), the majority of TCs in the North Atlantic form in the main development region (MDR) from seed disturbances called African easterly waves (AEWs; Russell et al. (2017)) that arise from instability of the mid-level African easterly jet. Factors influencing the frequency and strength of AEWs, either by modifying the strength of the African easterly jet – such as the West African Monsoon (WAM) – or modifying the environmental conditions that support the development of AEWs, represent another important source of variability in TC activity. It has been shown that convectively-coupled Kelvin waves (KWs) can influence TC activity by modulating the large-scale environment and promoting the evo-

lution of AEWs (e.g. Schreck (2016); Lawton et al. (2022)), affecting the likelihood of cyclogenesis. The development of AEWs is influenced by other environmental factors: deep convection can be suppressed by dry air from the Sahara desert that is carried into the Atlantic, and the warm SSTs needed to drive cyclogenesis are influenced by small-scale SST patterns that are coupled with low-level trade winds and circulation patterns (Kim et al., 2023). Finally, the Madden-Julian Oscillation (MJO) is the leading mode of intraseasonal variability in the tropics globally, which influences TC activity throughout the Atlantic basin (Maloney & Hartmann, 2000; Klotzbach & Oliver, 2015). Although the eastward-propagating convective patterns associated with the MJO are confined to the western Pacific, upper-tropospheric wind anomalies propagate around the globe that can temporarily enhance upper-level divergence over the North Atlantic basin, favouring cyclogenesis (Barrett & Leslie, 2009).

In this paper we review the factors that influenced activity during the 2025 North Atlantic hurricane season. The 2025 season is an interesting case study since common sources of variability such as ENSO and the MJO were weak, allowing other factors to more strongly drive changes in TC activity. ENSO conditions transitioned from neutral to weak La Niña during the season (NOAA, 2025), and the number of days with favourable MJO conditions in the North Atlantic during the Atlantic season (June to November) was the second lowest since 1991 according to the RMM index (Wheeler & Hendon, 2004). The 2025 season also saw the fifth warmest seasonal-mean daily SSTs in the MDR (using the OISST dataset; Huang et al. (2021)) yet ended with only slightly above-average activity (using HURDAT2; Landsea & Franklin (2013)). In an average Atlantic hurricane season, there are fourteen named storms, of which seven become hurricanes and three reach major hurricane status (NHC, 2026). In 2025, there were thirteen named storms, five hurricanes. It is therefore valuable to examine why 2025 was comparatively less active. Finally, it is noteworthy that most activity occurred in just four storms that reached major hurricane status, especially considering that three of the five hurricanes in 2025 reached category 5, the most since 2005 – an extremely active season. Although projections of TC activity in the changing climate are uncertain, the 2025 season appears to fit the model-predicted trend of decreasing overall activity alongside increasing intensity of individual TCs (Knutson et al., 2020).

In this study we identify which of the common drivers of TC activity in a typical season were more or less influential in the 2025 season, identify other factors that were more influential in 2025, and seek to explain the relative lack of activity in the context of above-average SSTs. As a single-season analysis, this study cannot directly attribute TC activity to individual drivers. Instead, we identify differences between periods with a relative change in activity within the season. Overall, reviewing the driving factors of a single season in this way is valuable as a case study of theoretical or statistical relationships identified in the literature, such as the influence of KWs on AEW development. In section 2 we summarise the 2025 North Atlantic hurricane season, review the state of the dominant drivers (SSTs and ENSO) and identify the unusual qualities of the 2025 season. The large-scale environmental conditions in the North Atlantic are addressed in section 3. In section 4 we explore AEWs in the 2025 season and, in particular, the influence of KWs and favourable MJO phases. Other sources of intraseasonal variability in 2025 are discussed in section 5 and we present our conclusions in section 6.

## 2 Season overview

Figure 1 shows TC tracks from the 2025 season and regional boxes used in later analysis. Climatologically, the Atlantic hurricane season lasts from 1 June to 30 November, with peak activity during August and September. In 2025, activity began on 23 June with three early short-lived tropical storms in the east of the basin but otherwise little activity throughout July and early August. Approaching the climatological peak, activity restarted when Hurricane Erin formed on 11 August and went on to reach category

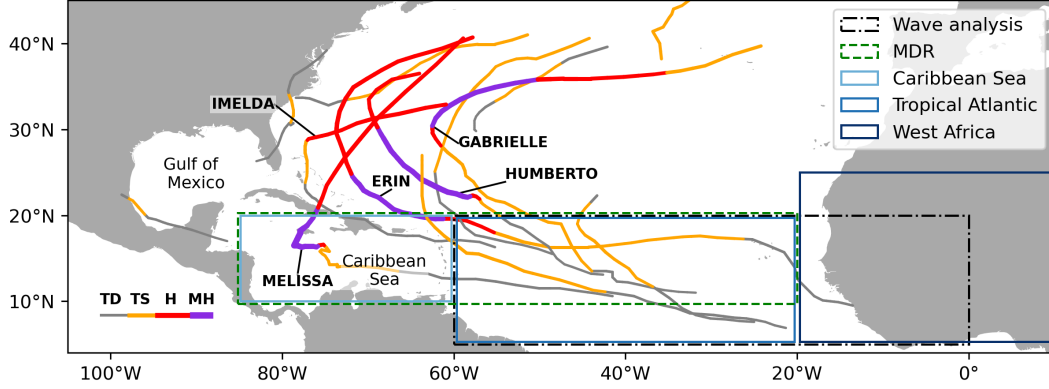


**Figure 1.** Summary map of the Atlantic basin, 2025 TC tracks, and region definitions used in this paper. Tracks are coloured by category (tropical depression TD; tropical storm TS; hurricane H; major hurricane MH) with line width proportional to maximum sustained wind speed. Hurricanes labelled. Coloured boxes indicate the MDR used in figure 2, wave analysis region used in figures 5 and 6, and the Caribbean Sea, Tropical Atlantic and West Africa regions used in figure 6. Track data for 2025 obtained from ATCF realtime (Sampson & Schrader, 2000).

5 strength. Thereafter, TC activity ceased throughout much of the peak season, similar to the lull observed in 2024 (Klotzbach et al., 2025). Two late-season clusters of activity brought cumulative season activity to above-average levels, again similar to the back-loaded 2024 season. In mid-late September, Hurricanes Gabrielle, Humberto, and Imelda formed, though none made landfall. In late October, Hurricane Melissa became the third category 5 hurricane of the season and the joint-strongest landfalling Atlantic hurricane with a maximum sustained wind speed of 185mph and central pressure of 892 hPa at landfall. Post-season analysis has verified a wind gust reading of 252 mph via dropsonde (UCAR, 2025), setting a new global record for the strongest dropsonde-measured wind gust in a TC.

SSTs are the strongest indicator of TC activity; the record-breaking 2005 season ( $ACE \sim 240$ ) was widely attributed to (at the time) record-warm SSTs (e.g. Trenberth & Shea (2006)) and a long-term increase in TC activity since 1994 has been attributed to a warm phase of the Atlantic Multidecadal Oscillation (e.g. Goldenberg et al. (2001)). The 2023 and 2024 Atlantic hurricane seasons saw record high SSTs throughout the Atlantic basin, surpassing 2005 – see figure 2, which shows daily-mean SSTs in the MDR from 1991–2020, with 2023, 2024, and 2025 highlighted. Despite the unprecedented temperatures, the 2024 season was remarkably quiet during the peak season (Klotzbach et al., 2025) owing to a northward shift in the track of AEWs, as well as strong vertical wind shear and broad-scale subsidence. Nonetheless, the season ended with above-average accumulated cyclone energy (ACE) owing to a late-season cluster of activity including two major hurricanes. Activity in the 2023 season was near-average, as El Niño conditions suppressed cyclogenesis. In 2025, MDR SSTs remained well above the long-term average. Daily-mean MDR SST anomalies (relative to 1991–2020 climatology) averaged  $0.47^\circ\text{C}$  during the 2025 hurricane season, making it the fifth-warmest on record. Alongside warm SSTs, five of the past six seasons have seen La Niña conditions during the peak season according to the relative Oceanic Niño Index (Climate Prediction Center, 2026b), although the La Niña signal was weak until late in 2025 season.

The 2025 season was unusual in the sense that activity was intermittent, with extended quiet periods separated by just three clusters of activity that featured particularly intense TCs. The total number of storms was close to average, the number of hur-

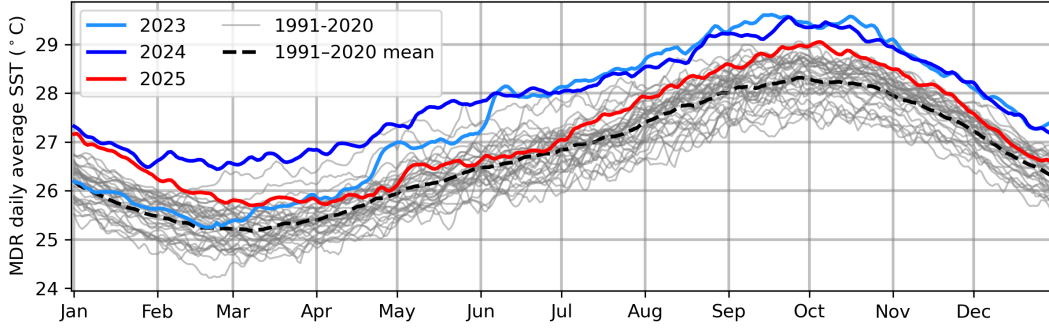


**Figure 2.** Daily-mean SSTs ( $^{\circ}$  C) in the Atlantic MDR ( $10\text{--}20^{\circ}$  N,  $20\text{--}85^{\circ}$  W) in 2023–2025 (coloured), compared with 1991–2020 climatology (grey, mean in dashed black). Data obtained from NOAA OISSTv2.1 (Huang et al., 2021).

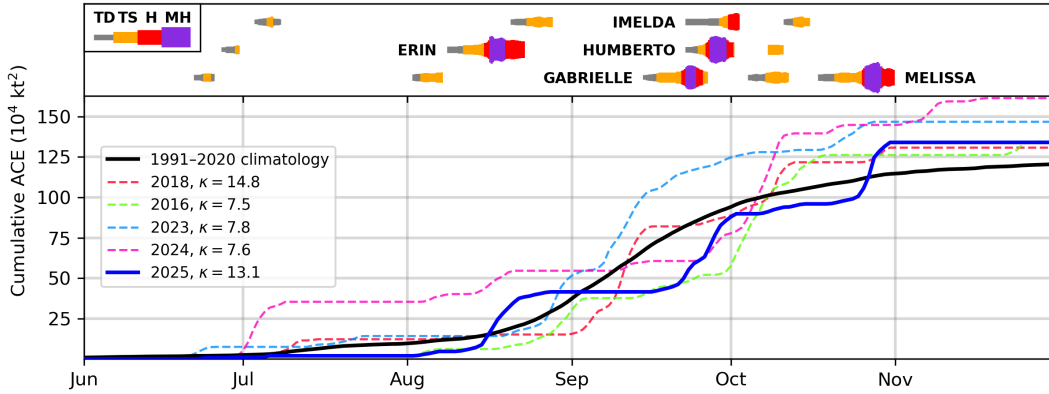


**Figure 3.** Cumulative Accumulated Cyclone Energy (ACE) in 2025 compared with the long-term (1991–2020) average and specific comparison years referred to in the text. Lifecycles of 2025 TCs inset, coloured as in figure 1, with hurricanes labelled. Data for 2025 obtained from ATCF realtime (Sampson & Schrader, 2000) and for 1991–2020 from HURDAT2 (Landsea & Franklin, 2013).

ricanes below average, but the number of major hurricanes above average. The season ended with a total accumulated cyclone energy (ACE) of  $132.5 (10^4 \text{ kt}^2)$ ; a measure of activity that combines the strength and duration of storms. Figure 3 shows the cumulative ACE in the 2025 season compared to 1991–2020 climatology, alongside a timeline of the season, clearly showing the three periods in which most of the cumulative ACE was generated. Comparison seasons (discussed below) are also shown. The 2025 season is classified as ‘above-normal’ according to the NOAA definition (based on % of the 1951–2020 median), consistent with the number of strong TCs observed. However, the classification is contradicted by the near-average number of storms and long periods of no/weak activity. The intermittency of the season is demonstrated by the fact that around 85% of the total season ACE occurred in just four out of thirteen storms. As noted earlier, this appears consistent with projected trends in TC activity as the climate warms (Knutson et al., 2020).

Another measure of intermittency is the kurtosis  $\kappa$  of the daily ACE distribution (using HURDAT2; Landsea & Franklin (2013)), which measures the tailedness of the distribution (Wilks, 2006): increasing values correspond to increasingly extreme deviations from the mean. In the modern climatology period from 1991 onwards, the 2025 season

is uniquely placed as an intermittent season with near-normal ACE (within 20% of the mean  $\sim 120$ ) and warm MDR SSTs. The 2025 ACE distribution has the second-highest kurtosis ( $\kappa \approx 13$ ) in this period (with mean  $\kappa \approx 7$ ), exceeded only by the 2018 season ( $\kappa \approx 15$ ). However, MDR SSTs in 2018 were below average ( $-0.28^\circ\text{C}$ ), with neutral ENSO conditions developing into El Niño late in the season, and a strong WAM (NOAA, 2026). The intermittency in 2018 can therefore be attributed to the frequent but relatively weak activity amid otherwise unfavourable conditions for TC activity, punctuated by a category 5 and a long-lived category 4 hurricane which generated extreme ACE values compared to the rest of the season, increasing  $\kappa$ . The near-normal ACE in 2018 exceeded expectations based on SSTs, whereas in 2025 the near-normal ACE can be viewed as unusual based on SSTs. Only the 2016 season has comparable MDR SSTs to 2025 ( $0.39^\circ\text{C}$ ) and near-normal ACE ( $\sim 140$ ) in the modern climatology period, but with near-average kurtosis ( $\kappa \approx 8$ ) indicating steady accumulation of ACE throughout the season amid favourable La Niña conditions. All other seasons with similar or greater SSTs (2005, 2010, 2017, 2020, 2023, 2024) saw well above-average activity, with the exception of 2023 which featured a strong El Niño. In the following sections we identify the unfavourable conditions that led to the relative lack of TC activity in 2025 and discuss factors that contributed to the strong intraseasonal variability compared to recent climatology, manifested as clusters of very active days interspersed with extended inactive periods.

### 3 Large-scale environmental conditions

The large-scale thermodynamic environment in the Atlantic basin in 2025 was generally unfavourable for TC activity. Figure 4 shows anomalies of four key environmental factors, averaged over the quiet early season (June and July) and the more active peak season (August to October). The latter period includes the peak-season lull from mid-August to mid-September, though the remainder of the period was more active. We consider sea-level pressure (SLP), relative SSTs (relative to the mean SST in the tropical belt  $20^\circ\text{N-S}$ ), 200–850 hPa temperature lapse-rate, and mid-level RH at 500 hPa. These factors act to favour or suppress cyclogenesis by providing or disrupting large-scale support for convection. Note that figure 4 shows a large-scale and time-averaged picture of the environment; localised support for cyclogenesis can – and did – drive convection over short periods. Moreover, there is a two-way feedback between TCs and their surrounding environment: TCs are associated with low SLP, extended regions of moist mid-level air, and tend to leave a cool SST wake in their path (Karnauskas et al., 2021). To account for contamination of the monthly average by strong long-lived TCs, we remove days with daily ACE exceeding 1 unit (0 days in June–July, 28 days in August–October).

The 2025 season saw basin-wide high SLP throughout. The typical pressure pattern in the Atlantic basin during the summer months features a subtropical high pressure system that drives the easterly trade winds in the tropics. Anomalous high summertime SLP (figure 4(a, b)) has been linked to suppressed TC activity owing to increased large-scale subsidence of air that dries out the mid-troposphere, as well as indicating the presence of a persistent tropical upper-tropospheric trough (TUTT) that increases vertical wind shear (see TUTT discussion in section 5; (Knaff, 1997)). High mid-level humidity (figure 4(c, d)) is essential to support deep convection; a dry mid-troposphere therefore reduces the likelihood of cyclogenesis, acting as a positive feedback loop that maintains the SLP anomaly. Although the dry anomalies are smaller-scale than the basin-wide high SLP, they are focussed in the tropical Atlantic near the coast of West Africa in June & July. These anomalies are also indicative of the dry Saharan air layer (SAL) extending into the Atlantic, disrupting the development of AEWs (see section 4). Examining differences between June, July and August (not shown) shows a wet/dry dipole that moves northward from the Guinea Coast (southern coast of West Africa) in June to the Sahel in central West Africa in July and August, indicating a gradual onset of the

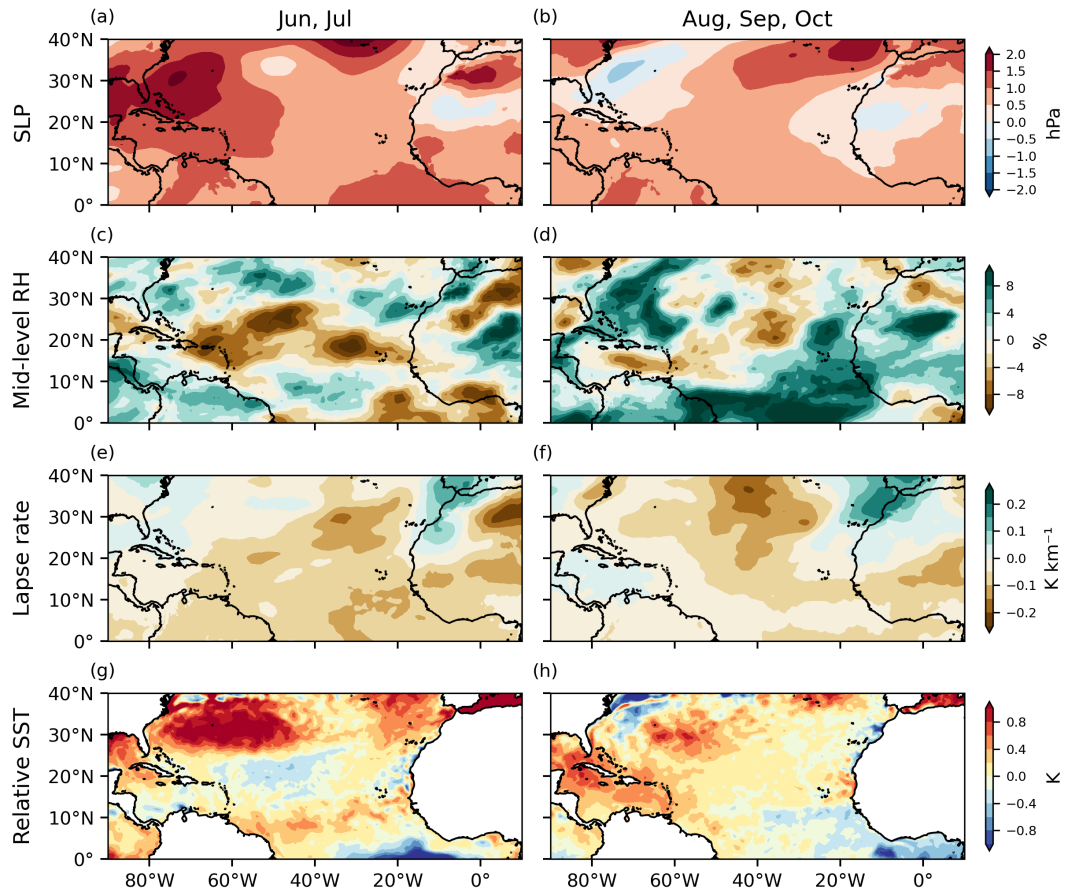


**Figure 4.** Monthly-mean anomaly (relative to 1991–2020 climatology) in June–July and August–October 2025 of (a, b) sea-level pressure, (c, d) 500 hPa relative humidity, (e, f) 850–200 hPa temperature lapse rate, and (g, h) relative sea surface temperature. Days with ACE greater than 1 are removed from the averages. Data from preliminary ERA5 reanalysis (Hersbach et al., 2020).

WAM that usually occurs in late June (e.g. Vellinga et al. (2013)). The position and strength of the convectively active region of the WAM is a crucial factor in the generation of AEWs (Hsieh & Cook, 2005). The weak WAM and high SLP both result in weak AEWs that are less likely to form TCs during July and early August. Although the high SLP anomaly persists in August–October, the anomaly is weaker and lower SLP is present near the US west coast. Correspondingly, the tropical Atlantic mid-troposphere is generally wetter than climatology during August–October, indicating a less hostile environment for AEWs and TC development.

Another persistent feature of the 2025 season is low temperature lapse-rates (figure 4(e, f), indicating a more stable atmosphere that is less favourable for deep convection. This is consistent with climate model predictions that lapse rates will decrease as the upper troposphere warms faster than the lower troposphere (e.g. Keil et al. (2021)), resulting in increasingly hostile thermodynamic conditions for TC development and intensification. Although the troposphere was more stable throughout the season (particularly over West Africa, likely disrupting the WAM), the tropical Atlantic and Caribbean Sea became less stable in August–October, providing better support for the development of TCs. The spatial pattern of SSTs throughout the 2025 season also acted against the development of convective systems in the Atlantic basin. This is best understood using relative SST anomalies (figure 4(g, h), with the mean SST anomaly in the tropical belt (20° S to 20° N) subtracted. Relative SSTs more clearly indicate patterns that can drive convection since warm SSTs are less effective when the surroundings are also warm (e.g. Williams et al. (2023)). Although SSTs remained close to record warmth in the MDR (figure 2), large parts of the Atlantic basin were also much warmer than average. In particular, the highest relative SST anomalies were found in the subtropical Atlantic, around 15° N. In a typical season, the Hadley cell circulation shifts slightly north of the equator during the summer months, with air rising in the tropics along the inter-tropical convergence zone (ITCZ) and sinking in the subtropics. Warmer SSTs in the subtropics are indicative of a weaker Hadley cell circulation that is less supportive of convection in the tropical Atlantic. The relative SST contrast between the tropics and subtropics was weaker in August–October compared to June and July. Other SST and circulation patterns played a role in the observed variability in activity during these months, such as the marked increase in SSTs in the Caribbean Sea that created a potent environment for category 5 Melissa to form and rapidly intensify in October (see section 5).

#### 4 Influence of Kelvin waves, MJO and WAM on African easterly waves

Russell et al. (2017) showed that 71% of North Atlantic TCs are linked to AEWs. Recent work has shown that KWs can support cyclogenesis by preconditioning the environment around AEWs (Lawton et al., 2022; Lawton & Majumdar, 2023), and the convectively active phase of a KW has been shown to modulate synoptic-scale conditions that favour the development of TCs from AEWs in the days following its passage (Rios-Berrios, Tang, et al., 2024). The MJO has also been shown to favour cyclogenesis during periods of anomalous upper-level divergence (Barrett & Leslie, 2009). We emphasise that KWs and the MJO do not directly initiate cyclogenesis, rather they influence AEW development, thereby increasing the likelihood of cyclogenesis. Here we analyse AEWs in the 2025 Atlantic season using the lower-troposphere (700 hPa) relative vorticity anomaly  $\zeta'$  (e.g. Jonville, Cornillault, et al. (2025)). AEWs are identified as positive  $\zeta'$  values following a bandpass filter with period 2–6 days (e.g. Hopsch et al. (2010)) and wavenumbers 6–20 (e.g. Schreck et al. (2012)). To explore the role of MJO favourable periods we use a bandpass filter with period 30–96 days and wavenumbers 1–5 applied to the velocity potential anomaly at 200 hPa,  $\chi_{200}$ , with negative values corresponding to divergence in the upper troposphere. Similarly, the role of KWs is investigated using a bandpass filter with period 2.5–20 days, wavenumbers 1–14, and equivalent depths 8–90 m applied to outgoing long-wave radiation (OLR) anomaly; negative values corre-

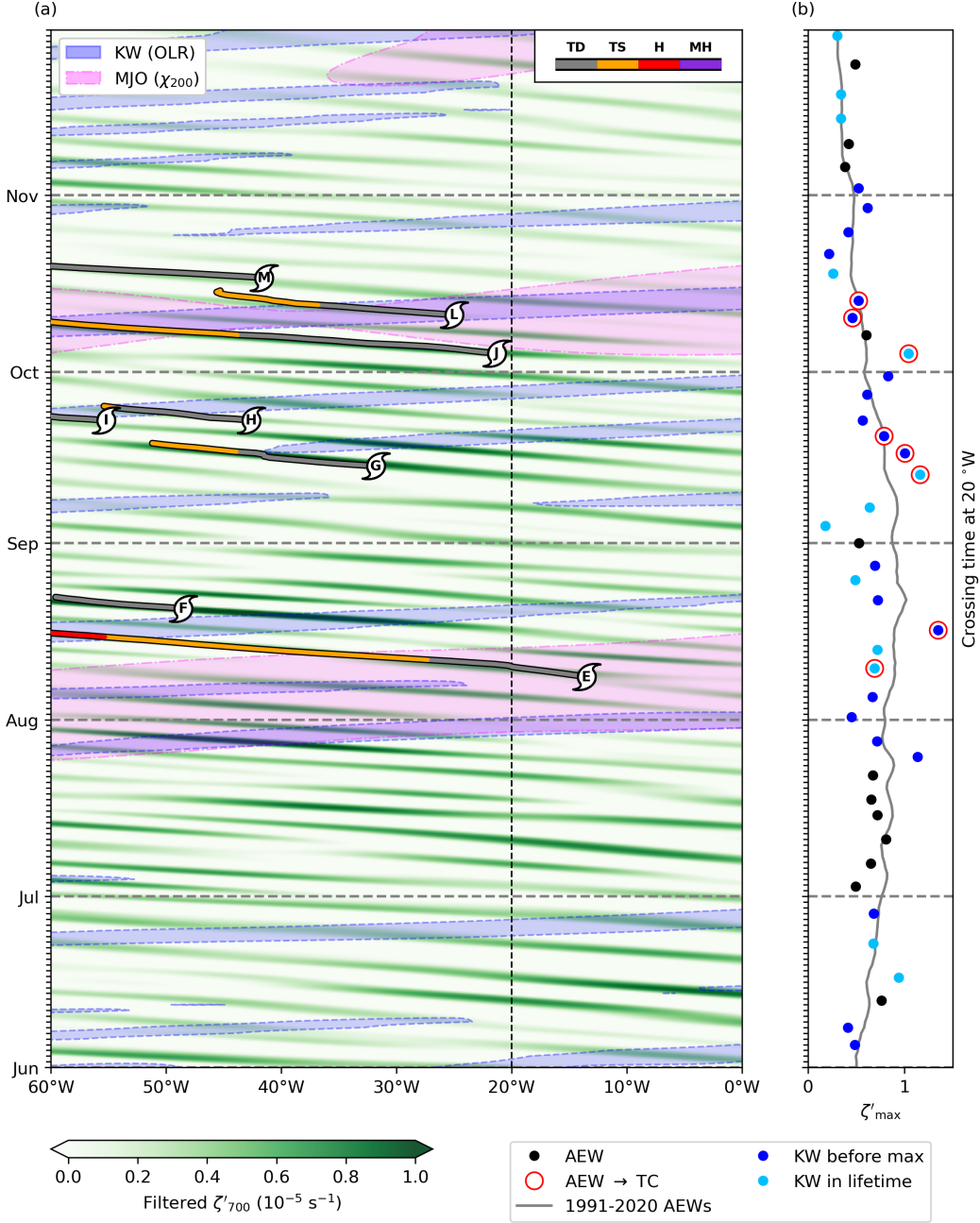


**Figure 5.** (a) Hovmöller plot of the AEW-filtered relative vorticity anomaly  $\zeta'$  (relative to 1991–2020 climatology) at 700 hPa averaged over 5–20°N latitude. Only positive values are shown for clarity. Favourable KW (MJO) signals are shown where the filtered OLR anomaly (velocity potential anomaly at 200 hPa) is more than one standard deviation below the mean. TC tracks are overlaid where TCs are within the wave analysis region indicated in figure 1. (b) AEW maximum amplitude (maximum relative vorticity anomaly  $\zeta'_{\max}$ ) versus crossing-time at 20°N. AEWs whose maximum amplitude occurs up to four days after a passing favourable KW signal are coloured blue. AEWs that form TCs are emphasised with a red circle. Data from preliminary ERA5 reanalysis (Hersbach et al., 2020) other than  $\chi_{200}$ : 2025 data from CFS (Schneider et al., 2013), climatology from NOAA PSL.

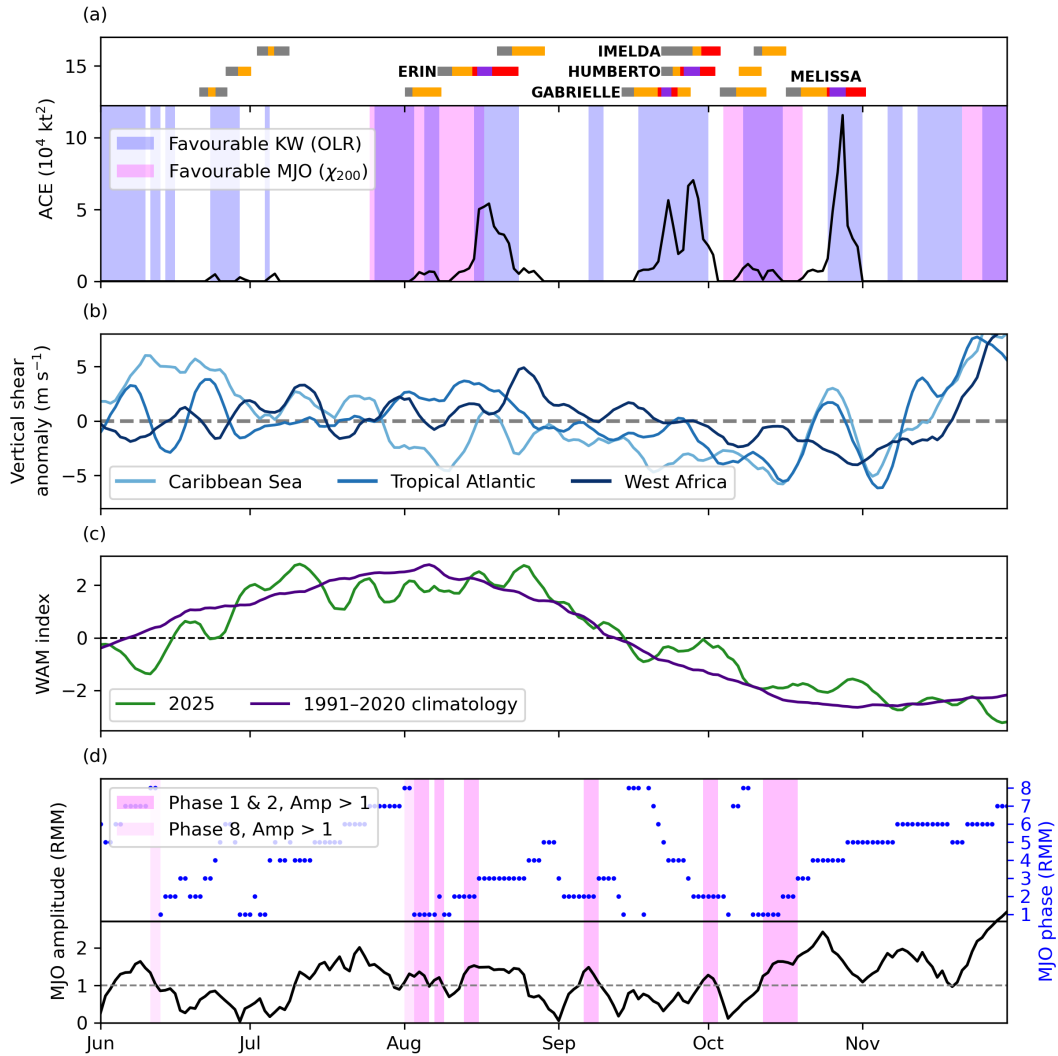
spond to convectively active KW phases (Ventrice, Thorncroft, & Schreck, 2012). A 40-day buffer period is added to the beginning and end of the time period of interest (June to November) to reduce spectral leakage. Favourable MJO conditions and KW phases are identified where the wave-filtered signal is less than one standard deviation below the mean (both calculated within the wave analysis region).

Figure 5(a) shows a Hovmöller plot (longitude vs. time) of the AEW-filtered, latitudinally-averaged  $\zeta'$  field in the wave analysis region ( $0\text{--}60^\circ\text{W}$ ,  $5\text{--}20^\circ\text{N}$ ) indicated in figure 1. TC tracks are overlaid whilst the TC remains in the wave analysis region and coloured by intensity as in figure 1. Convectively active KW phases and favourable MJO conditions are indicated by blue and magenta shading, respectively. To assess the varying strength of AEWs through the season, figure 5(b) shows the maximum relative vorticity anomaly  $\zeta'_{\max}$  along each AEW track compared to climatology, plotted at the time that the track passes  $20^\circ\text{W}$ , corresponding to the approximate time that the AEW crosses the West African coast into the Atlantic. AEWs that reach their maximum amplitude up to four days after the passage of a convectively active KW phase are highlighted in solid blue. The choice of lead-time is based on analysis of the time lag between cyclogenesis and KW peaks by Rios-Berrios, Tang, et al. (2024). AEWs that experience the passage of a KW in their lifetime are highlighted in light blue. AEWs that produce TCs are circled in red, using post-season analyses (NHC, 2026) for confirmation.

Whilst the number of AEWs crossing  $20^\circ\text{W}$  during the 2025 hurricane season (46) is close to the climatological average (43) when calculated using our method, the maximum amplitude of the AEWs is below average for extended periods that coincide with low TC activity in the Atlantic basin, particularly July and most of August. Whilst weaker-than-average AEWs can still develop into TCs (e.g. Erin in mid-August), they are more likely to be disrupted during their evolution, reducing the likelihood of cyclogenesis (Agudelo et al., 2011). Six of eight AEWs that produce TCs in 2025 are close to or stronger than the climatological average. The frequency of AEWs entering the Atlantic basin appears uniform throughout the season, but owing to the disrupted WAM (due to anomalous subsidence and increased stability) and dry air over West Africa noted in section 3 and shown below, AEWs were generally weaker and consequently less likely to produce TCs during the first half of the season.

Figure 5(b) shows that many TC-producing AEWs are influenced by KWs shortly before reaching their maximum amplitude, consistent with Rios-Berrios, Tang, et al. (2024), and periods with a lack of KW activity (e.g. July and mid-August to mid-September) coincide with periods with weak AEWs. The latter observation may have played a role in the relative lack of TC activity during these periods – Thorncroft & Hodges (2001) showed that variability in the amplitude of AEWs, not just the number of AEWs, can influence TC activity. Over the season, the influence of KWs was consistent with climatology: 74% of AEWs during the 2025 season were influenced by KWs at some point in their lifetime, consistent with results from Lawton & Majumdar (2023) that 76% of AEWs were KW-influenced in a 39 year record from 1981 to 2019.

The suppressed development of AEWs in June–August can also be linked to episodes of strong vertical shear, dry air and increased subsidence over the tropical Atlantic, preventing development of AEWs downstream of West Africa. Figure 6(a) shows a time-series of daily ACE highlighted where favourable MJO conditions and KW phases are present in the wave analysis region used in figure 5. Figure 6(b) shows the 850–200 hPa deep-layer vertical wind shear anomaly, regionally averaged in the Caribbean Sea, tropical Atlantic, and West Africa (as shown in figure 1). Thresholding of the 700 hPa relative vorticity anomaly shown in figure 5 was used to remove TCs and AEWs from the averages. Figure 6(b) shows that strong vertical shear was present for extended periods up to the middle of September in West Africa and the tropical Atlantic, disrupting the development of AEWs.



**Figure 6.** Timeseries of activity, vertical shear, WAM circulation strength, and favourable KW and MJO periods in the 2025 Atlantic hurricane season. (a) Daily ACE with periods of favourable MJO and KW activity highlighted in magenta and blue, respectively, corresponding to presence of favourable wave signals as shown in figure 5. Lifecycles of 2025 TCs shown with intensity indicated in colour as in figure 3. (b) Daily mean 850–200 hPa vertical wind shear anomaly in the Caribbean Sea, Tropical Atlantic and West Africa. Averaging regions shown in figure 1. (c) WAM circulation index, defined as in Ndiaye et al. (2009) (see text). (d) MJO amplitude and phase calculated from the Real-time Multivariate MJO (RMM) index (Wheeler & Hendon, 2004) provided by the Australian Bureau of Meteorology.

Figure 6(c) shows a WAM index defined as the standardised difference between the 925 hPa wind speed and the 200 hPa zonal wind speed averaged over 20°W–20°E, 3–13°N, following Ndiaye et al. (2009). The WAM index measures the strength of the monsoon circulation: the monsoon can be considered ‘active’ when the index is positive, though onset of the WAM is difficult to define objectively (Fitzpatrick et al., 2015). AEW amplitudes typically decrease as WAM weakens and dissipates in October, but the African easterly jet persists into November, continuing to produce weak AEWs (Afiesimama, 2007). Note that the circulation weakens in September whilst monsoon rainfall persists (Pu & Cook, 2012; Zhang & Cook, 2014), reducing the WAM index from September onwards as seen in the 1991–2020 climatology in figure 6(c), despite continued influence on AEWs. The WAM index is consistent with a disrupted WAM during the first half of the season (JJA) noted earlier, as well as a stronger WAM during late September and October.

One of the strongest sources of intraseasonal variability in TC activity in the Atlantic basin is the MJO. Typically, the MJO favours TC formation in the Atlantic basin when in phases one and two, when upper-level divergence is enhanced over the African continent and Indian Ocean (strengthening the WAM and African easterly jet, influencing AEW development) and to a lesser extent also phase eight (Klotzbach, 2010; Barnston et al., 2015). The phase and amplitude of the MJO is often characterised using the RMM index (Wheeler & Hendon, 2004) shown in figure 6(d); the MJO is considered ‘coherent’ when the RMM amplitude exceeds 1. Periods with a coherent and favourable MJO are highlighted, which are broadly consistent with the favourable periods identified via wave-filtering as shown in figure 5 and 6(a). On average in 1991–2020 there were 49 days during the Atlantic hurricane season where the MJO was coherent and in phase 1, 2, or 8, with a standard deviation of 13 days. In 2025, there were only 25 days with these favourable MJO conditions, the second lowest since 1991. Combined with the increased stability and high SLP throughout the 2025 season, the relative lack of favourable MJO conditions may have contributed to the lack of TC activity relative to expectations based on the warm SSTs. It can be seen from figures 5 and 6 that favourable MJO forcing occurred in two periods, coinciding with the development of TCs from AEWs: first, Erin and Fernando in mid-August, later, Lorenzo and Melissa in mid-October. The AEWs from which Fernando, Lorenzo and Melissa formed were also influenced by KWs.

## 5 Circulation and SST patterns

The relative lack of activity in the 2025 season can be viewed as a result of generally unfavourable large-scale conditions (SLP, stability), as well as disrupted AEW development early (June, July) and late (November) in the season owing to smaller-scale variability in conditions (shear, humidity) and WAM strength. Here we discuss how the upper-level circulation as well as low-level trade winds and SST patterns contributed to the observed intraseasonal variability. In boreal summer months, the upper-level circulation pattern in the North Atlantic features a tropical upper-tropospheric trough (TUTT) adjacent to the subtropical (Azores) high. The strength, position and orientation of the TUTT is subject to internal variability as well as influence from mid-latitude wave-breaking and TCs (Ferreira & Schubert, 1999; Lu et al., 2017). The TUTT can also influence TC genesis (Sears & Velden, 2014) and intensification (Fischer et al., 2017). The upper-level flow brings cold air from the mid-latitudes into the subtropics, increasing lapse-rates that favour convection, as well as enhancing divergence equatorward and east of the trough. However, the strong upper-level winds can also increase deep-layer shear and, depending on extent and position, mix dry subtropical air into the tropics and draw the SAL into the tropical Atlantic, suppressing TC activity. The movement of TCs is also heavily influenced by upper atmospheric winds that act as a ‘steering flow’, meaning a TUTT can promote recurvature in the mid-Atlantic.

Figure 7 shows monthly-mean upper-tropospheric winds and geopotential height contours in the Atlantic basin from June to September, with upper-level troughs indi-

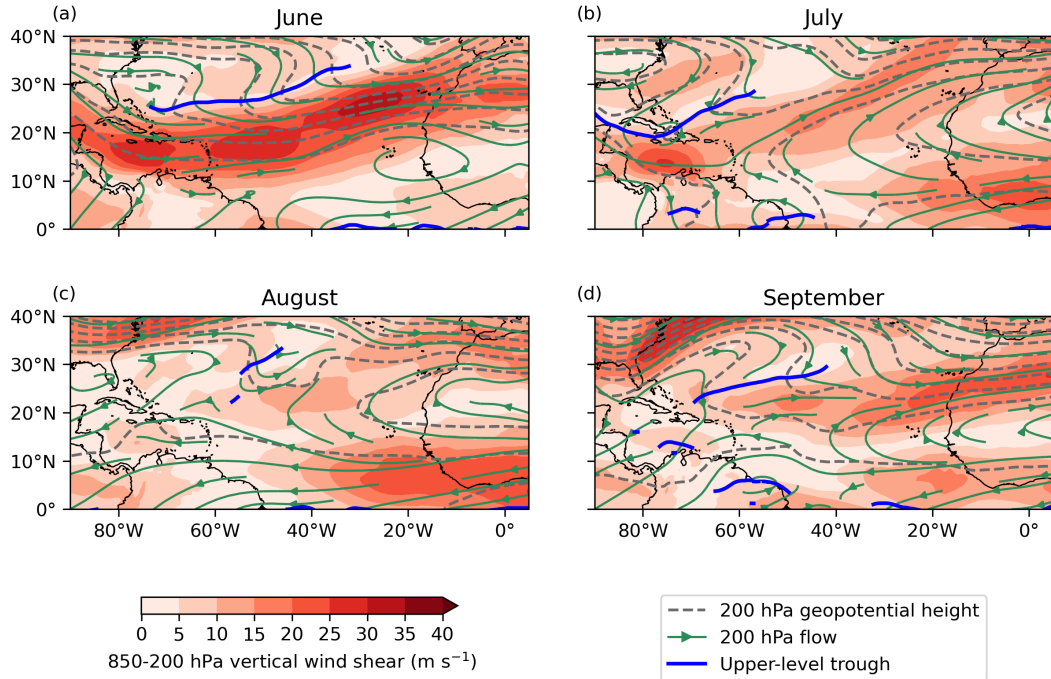


**Figure 7.** Upper-troposphere (200 hPa) geopotential height contours (grey dashed, 30 m interval) and flow streamlines (green) with 850–200 hPa vertical shear (coloured) in June to September 2025. Troughs are indicated by thick blue lines. Data from preliminary ERA5 reanalysis (Hersbach et al., 2020).

cated by blue lines, illustrating the persistent TUTT present in June and July that contributed to the strong vertical shear and dry tropical Atlantic noted in sections 3 and 4. Although the TUTT weakened in August, strong vertical shear was still present near West Africa that likely continued to disrupt AEW development. In September, the TUTT regained strength but with more favourable positioning and weaker shear that may have supported intensification of TCs moving westward across the Atlantic. Owing to the two-way feedback between TCs and TUTTs, figure 7 does not exclude days with large ACE values unlike figure 3. It is possible that the increase in TC activity in September contributed to variability in the TUTT: note that Imelda and Humberto formed between 40–60°W, close to the trough axis.

It is notable that most TCs remained well offshore this season. The exceptions are Barry and Chantal, which made landfall in the US as tropical storms early in the season, and Melissa, which made landfall in Jamaica at peak strength as a category 5 major hurricane and later in Cuba as a category 3. Although the TUTT varied in strength through the season, the upper-level circulation pattern favoured recurving TCs throughout. Persistent low SLP near the US coast in August–October also likely contributed to the recurvature of TCs (see figure 4(b)).

Variability in SST patterns and low-level winds can influence TC activity by shifting convection patterns such as the ITCZ via changes in surface convergence and evaporation rates (Kossin & Vimont, 2007; Wang et al., 2025). Figure 8 shows the 10 m wind speed anomaly (a, b) and SST anomaly (c, d). Low-level 10 m trade winds are overlaid. Days with ACE > 1 are excluded as in figure 4. Surface convergence zones in 2025 and 1991–2020 climatology are shown using a simplified version of the Berry & Reeder (2014) methodology that identifies convex minima in the 925 hPa convergence field. The dom-

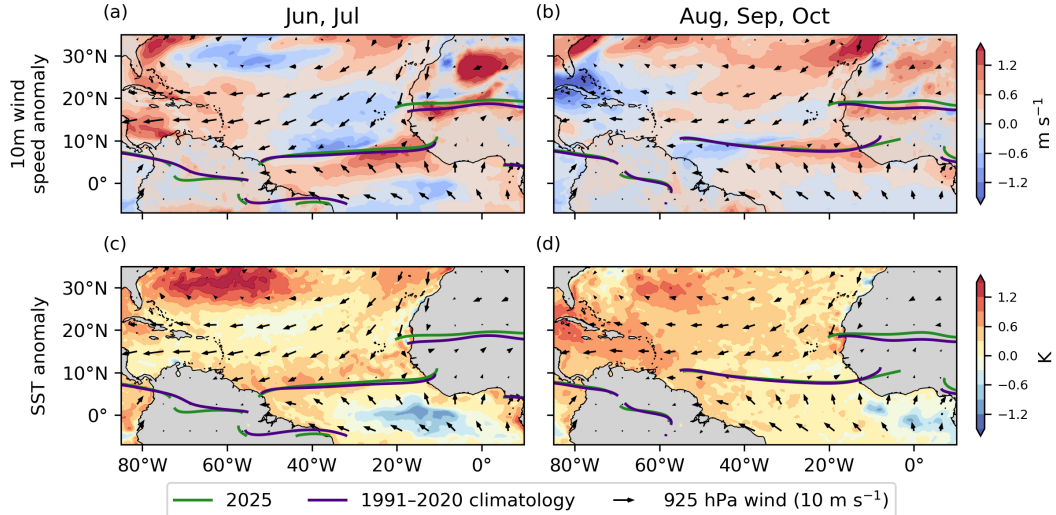


**Figure 8.** Low-level (10m) winds overlaid on 10m wind speed anomaly (top row, colour) and SST anomaly (bottom row, colour) relative to 1991–2020 climatology. Position of the ITCZ indicated by lines of convergence at 925 hPa in 2025 (green) and 1991–2020 climatology (purple) using a modified version of the Berry & Reeder (2014) methodology. Data from preliminary ERA5 reanalysis (Hersbach et al., 2020).

inant mode of interannual variability in tropical SSTs is the Atlantic equatorial mode (AEM), also referred to as the Atlantic zonal mode or Atlantic Niño (Niña) in the positive (negative) phase (Dippe et al., 2019). The AEM tends to develop in late boreal spring, peaking in May to July, and is closely related to the formation of a ‘cold-tongue’ of cooler-than-average SSTs in the eastern equatorial Atlantic during the negative phase (Keenlyside & Latif, 2007; Dippe et al., 2018). In the warm phase (Atlantic Niño), the AEM strengthens the ITCZ and WAM, increasing AEW activity and surface convergence in the tropical eastern Atlantic (Kim et al., 2023). Conversely, the presence of an equatorial cold-tongue during the cold phase (Atlantic Niña) can weaken the WAM as a result of the reduced temperature gradient between the Gulf of Guinea and the Sahel that drives the monsoon circulation (Okumura & Xie, 2004; Caniaux et al., 2011). A negative phase of the AEM (Atlantic Niña, the first since 2014) developed in June, lasting until August and returning to neutral from September onwards (Climate Prediction Center, 2026a). The negative-AEM associated equatorial cold-tongue is clearly seen between 0–30 °W in figure 8(c), consistent with a weakened WAM and disrupted AEW activity in June, July and much of August as noted in the analysis of AEWs in section 4. During August–October the cold-tongue is less pronounced (figure 8(d)).

The dominant mode of coupled SST/low-level wind variability in the Atlantic basin is the Atlantic meridional mode (AMM), characterised by a north-south dipole of SST and surface wind anomalies across the equator, which can influence TC activity via changes in the large-scale circulation (modifying shear) and shifts in the ITCZ position (Vimont & Kossin, 2007; Xia et al., 2023). In the 2025 season, the AMM index was strongly positive during September and October (Physical Sciences Laboratory, 2026). However, variability in the trade winds and ITCZ position shown in figure 8 are not clearly consistent with this index, and there is no clear dipole in SST anomalies, potentially as a result of the complex interactions between the AMM and AEM (Foltz & McPhaden, 2010) and weakening of the AMM after boreal spring (Amaya et al., 2017). A full analysis of this discrepancy is beyond our scope.

In June and July, the north-easterly trade winds between 60–20 °W were weak and the ITCZ was shifted slightly north. Although weakened trade winds typically weaken vertical shear, the anomalously strong upper-level winds counteracted this response (figure 7). In August–October, the Atlantic segment of the ITCZ was close to its climatological position but the West African segment (associated with the WAM) was still displaced northward, whilst the 60–20 °W trade winds were anomalously strong. The northward shifted convergence zone in West Africa likely resulted in a more northward track of AEWs. Stronger vertical wind shear (figure 7) and cooler SSTs (figure 8(c,d)) mean that AEWs on a northward shifted track tend to be weaker and therefore less likely to develop into TCs, as observed in 2024 (Klotzbach et al., 2025) and supported by the generally low AEW amplitudes noted in section 4. The increasing strength of the trade winds may have contributed to the cooler SSTs in the 5–15 °N belt by increasing surface evaporation rates from the early to late season. Similarly, the weakening trade winds in the Caribbean Sea from early to late season (compare figure 8(d) and (c)) likely contributed to the increase in SSTs in the region (noted in section 3).

## 6 Conclusion

The 2025 Atlantic hurricane season was near-normal in terms of cumulative ACE relative to the recent climatology period from 1991 onwards, despite weakly favourable La Niña conditions and above-average SSTs in the MDR that in previous seasons have led to above-average activity. The 2025 season was the second most intermittent of all seasons since 1991 with near-normal activity; the majority of ACE was produced by four major hurricanes out of a total of thirteen named storms. In this sense, the 2025 season fits into the model-predicted trend of decreasing activity alongside increasing intensity of individual TCs (Knutson et al., 2020).

In this paper we discussed the factors that influenced the 2025 season, identifying unfavourable large-scale conditions in the form of high SLP and increased atmospheric stability throughout. The early season (June and July) was quiet owing to a disrupted WAM, resulting in weak AEWs (diagnosed using wave-filtered relative vorticity) that were not able to develop in the Atlantic basin. Strong vertical shear and an extended dry air layer near West Africa from a persistent strong TUTT also disrupted AEWs during this period. Stronger AEWs moving into the Atlantic basin during August, likely supported by an increase in KW activity and favourable MJO conditions, led to an increase in activity with the first major hurricane of the season (Erin). During the climatological peak of the hurricane season, from mid August to mid September, no activity occurred. Vertical shear, unfavourable circulation and SST patterns from an Atlantic Niña event, and strong subsidence disrupted the development of AEWs and suppressed cyclogenesis. September and October saw two further clusters of activity as vertical shear weakened and the WAM regained strength. Hurricanes Gabrielle, Humberto and Imelda all formed and reached peak strength during a two week period in late September. The restrengthened and more favourably positioned TUTT, as well as more frequent KW activity, may have supported the development of AEWs crossing the Atlantic basin. The final burst of activity in October coincided with favourable MJO conditions, during which Melissa formed and later developed into an intense category 5 hurricane owing to particularly warm SSTs in the Caribbean Sea that were aided by weakened trade winds in the preceding months.

Recent research showing that convectively active KW phases can modulate the development of AEWs is supported by the analysis presented in section 4 (Lawton & Majumdar, 2023; Rios-Berrios, Tang, et al., 2024). The analysis presented in this study represents an addition to recent case studies of KW influence on cyclogenesis using observations (Ventrice, Thorncroft, & Janiga, 2012; Jonville, Borne, et al., 2025) and modelling (Chien et al., 2026). The extended periods of low activity in the 2025 season coincided with an absence of KW activity, particularly in July. Compared to recent cli-

matology, there were also relatively few episodes of favourable MJO conditions. The factors that influence KW and MJO variability were not studied here but represent an important topic for future research, particularly their predictability. Further, it remains an open question whether KW influence on the development of AEWs and modulation of the large-scale environment by the MJO will become more important in a future climate with a more stable Atlantic. Other aspects of predictability that could be explored in future work include the persistence of TUTTs, which played a key role in controlling vertical wind shear in the 2025 season, and the interactions between different modes of variability in SST patterns such as the AEM which appeared to ‘mask’ the typical AMM response in 2025.

Many interesting aspects of the 2025 season have not been covered in this study. One key aspect is rapid intensification (RI): in the North Atlantic, around 80% of TCs that undergo RI become major hurricanes and there is evidence that RI is becoming more common (Bhatia et al., 2019). There were several examples of RI observed this season as the major hurricanes developed, which appears to support that trend. Another aspect is the continued advancement of AI tracking and intensity models, some of which appeared to pick up on episodes of RI ahead of conventional physical models (NHC, 2025).

## Data availability statement

Scripts used to generate the figures in this manuscript can be found at [https://github.com/qntmCharles/retro\\_2025](https://github.com/qntmCharles/retro_2025). The following datasets have been used:

- Optimum Interpolation SST (OISSTv2.1), available from the National Oceanic and Atmospheric Administration (NOAA) (<https://www.ncei.noaa.gov/products/optimum-interpolation-sst>)
- Atlantic Hurricane Database (HURDAT2), available from the National Hurricane Center (NHC) (<https://www.nhc.noaa.gov/data/hurdat/>)
- Automated Tropical Cyclone Forecast (ATCF) system best-track (btk) files, available from the NHC FTP server (<https://ftp.nhc.noaa.gov/atcf/btk/>)
- Fifth generation of ECMWF atmospheric reanalyses of the global climate (ERA, preliminary), obtained from the Copernicus Climate Change Service (C3S) (<https://cds.climate.copernicus.eu>)
- Climate Forecast System (CFS) reanalysis, available from the National Centre for Atmospheric Research (NCAR) (<https://climatedataguide.ucar.edu/climate-data/climate-forecast-system-reanalysis-cfsr>)
- MJO RMM index data provided by the Australian Bureau of Meteorology (<https://www.bom.gov.au/climate/mjo/>)
- NOAA Physical Sciences Laboratory (PSL) (<https://psl.noaa.gov/>)

## Acknowledgements

This project is supported by Inigo Limited. The author is grateful for insightful comments from Alison Ming, Ruth Petrie, Sebastian Schemm and two anonymous reviewers during preparation of this manuscript.

## Author Contributions

Charles Powell: Conceptualization; formal analysis; visualization; writing – original draft; writing – review & editing.

## References

- Afiesimama, E. A. (2007, September). Annual cycle of the mid-tropospheric easterly jet over West Africa. *Theor. Appl. Climatol.*, *90*(1-2), 103–111. doi: 10.1007/s00704-006-0284-y
- Agudelo, P. A., Hoyos, C. D., Curry, J. A., & Webster, P. J. (2011, April). Probabilistic discrimination between large-scale environments of intensifying and decaying African Easterly Waves. *Clim Dyn*, *36*(7-8), 1379–1401. doi: 10.1007/s00382-010-0851-x
- Amaya, D. J., DeFlorio, M. J., Miller, A. J., & Xie, S.-P. (2017, September). WES feedback and the Atlantic Meridional Mode: Observations and CMIP5 comparisons. *Clim Dyn*, *49*(5-6), 1665–1679. doi: 10.1007/s00382-016-3411-1
- Barnston, A. G., Vigaud, N., Long, L. N., Tippett, M. K., & Schemm, J.-K. E. (2015, December). Atlantic Tropical Cyclone Activity in Response to the MJO in NOAA’s CFS Model. *Mon. Weather Rev.*, *143*(12), 4905–4927. doi: 10.1175/MWR-D-15-0127.1
- Barrett, B. S., & Leslie, L. M. (2009, February). Links between Tropical Cyclone Activity and Madden–Julian Oscillation Phase in the North Atlantic and Northeast Pacific Basins. *Mon. Weather Rev.*, *137*(2), 727–744. doi: 10.1175/2008MWR2602.1
- Berry, G., & Reeder, M. J. (2014, March). Objective Identification of the Intertropical Convergence Zone: Climatology and Trends from the ERA-Interim. *J. Clim.*, *27*(5), 1894–1909. doi: 10.1175/JCLI-D-13-00339.1
- Bhatia, K. T., Vecchi, G. A., Knutson, T. R., Murakami, H., Kossin, J., Dixon, K. W., & Whitlock, C. E. (2019, February). Recent increases in tropical cyclone intensification rates. *Nat Commun*, *10*(1), 635. doi: 10.1038/s41467-019-08471-z
- Caniaux, G., Giordani, H., Redelsperger, J.-L., Guichard, F., Key, E., & Wade, M. (2011, April). Coupling between the Atlantic cold tongue and the West African monsoon in boreal spring and summer. *J. Geophys. Res.*, *116*(C4), C04003. doi: 10.1029/2010JC006570
- Chien, M.-T., Barnes, E. A., & Maloney, E. D. (2026, January). Modulation of Tropical Cyclogenesis by the Convectively Coupled Kelvin Waves: Insights From Data-Driven Climate Emulator ACE2. *Geophysical Research Letters*, *53*(2), e2025GL117387. doi: 10.1029/2025GL117387
- Climate Prediction Center, N. (2026a). *Atlantic 3 Index*. [https://www.cpc.ncep.noaa.gov/products/international/ocean\\_monitoring/IODMI/ATL3\\_month.html](https://www.cpc.ncep.noaa.gov/products/international/ocean_monitoring/IODMI/ATL3_month.html). (Accessed 13 February 2026.)
- Climate Prediction Center, N. (2026b). *Relative Oceanic Niño Index*. [https://www.cpc.ncep.noaa.gov/products/analysis\\_monitoring/enso/roni/](https://www.cpc.ncep.noaa.gov/products/analysis_monitoring/enso/roni/). (Accessed 17 February 2026.)
- Corporal-Lodangco, I. L., Richman, M. B., Leslie, L. M., & Lamb, P. J. (2014). Cluster Analysis of North Atlantic Tropical Cyclones. *Procedia Computer Science*, *36*, 293–300. doi: 10.1016/j.procs.2014.09.096
- Dippe, T., Greatbatch, R. J., & Ding, H. (2018, July). On the relationship between Atlantic Niño variability and ocean dynamics. *Clim Dyn*, *51*(1-2), 597–612. doi: 10.1007/s00382-017-3943-z
- Dippe, T., Greatbatch, R. J., & Ding, H. (2019, May). Seasonal prediction of equatorial Atlantic sea surface temperature using simple initialization and bias correction techniques. *Atmospheric Science Letters*, *20*(5), e898. doi: 10.1002/asl.898
- Emanuel, K. (2003, May). Tropical Cyclones. *Annu. Rev. Earth Planet. Sci.*, *31*(1), 75–104. doi: 10.1146/annurev.earth.31.100901.141259
- Ferreira, R. N., & Schubert, W. H. (1999, August). The Role of Tropical Cyclones in the Formation of Tropical Upper-Tropospheric Troughs. *J. Atmos. Sci.*, *56*(16), 2891–2907. doi: 10.1175/1520-0469(1999)056<2891:TROTTCI>2.0.CO;2

- Fischer, M. S., Tang, B. H., & Corbosiero, K. L. (2017, April). Assessing the Influence of Upper-Tropospheric Troughs on Tropical Cyclone Intensification Rates after Genesis. *Mon. Weather Rev.*, *145*(4), 1295–1313. doi: 10.1175/MWR-D-16-0275.1
- Fitzpatrick, R. G. J., Bain, C. L., Knippertz, P., Marsham, J. H., & Parker, D. J. (2015, November). The West African Monsoon Onset: A Concise Comparison of Definitions. *J. Clim.*, *28*(22), 8673–8694. doi: 10.1175/JCLI-D-15-0265.1
- Foltz, G. R., & McPhaden, M. J. (2010, September). Interaction between the Atlantic meridional and Niño modes. *Geophysical Research Letters*, *37*(18), 2010GL044001. doi: 10.1029/2010GL044001
- Goldenberg, S. B., Landsea, C. W., Mestas-Nuñez, A. M., & Gray, W. M. (2001, July). The Recent Increase in Atlantic Hurricane Activity: Causes and Implications. *Science*, *293*(5529), 474–479. doi: 10.1126/science.1060040
- Gray, W. M. (1968, October). GLOBAL VIEW OF THE ORIGIN OF TROPICAL DISTURBANCES AND STORMS. *Mon. Wea. Rev.*, *96*(10), 669–700. doi: 10.1175/1520-0493(1968)096<0669:GVOTOO>2.0.CO;2
- Gray, W. M. (1984, September). Atlantic Seasonal Hurricane Frequency. Part I: El Niño and 30 mb Quasi-Biennial Oscillation Influences. *Mon. Wea. Rev.*, *112*(9), 1649–1668. doi: 10.1175/1520-0493(1984)112<1649:ASHFPI>2.0.CO;2
- Hersbach, H., Bell, B., Berrisford, P., Hirahara, S., Horányi, A., Muñoz-Sabater, J., ... Thépaut, J.-N. (2020, July). The ERA5 global reanalysis. *Quart J Royal Meteor Soc*, *146*(730), 1999–2049. doi: 10.1002/qj.3803
- Hopsch, S. B., Thorncroft, C. D., & Tyle, K. R. (2010, April). Analysis of African Easterly Wave Structures and Their Role in Influencing Tropical Cyclogenesis. *Mon. Weather Rev.*, *138*(4), 1399–1419. doi: 10.1175/2009MWR2760.1
- Hsieh, J.-S., & Cook, K. H. (2005, May). Generation of African Easterly Wave Disturbances: Relationship to the African Easterly Jet. *Mon. Weather Rev.*, *133*(5), 1311–1327. doi: 10.1175/MWR2916.1
- Huang, B., Liu, C., Banzon, V., Freeman, E., Graham, G., Hankins, B., ... Zhang, H.-M. (2021, April). Improvements of the Daily Optimum Interpolation Sea Surface Temperature (DOISST) Version 2.1. *J. Clim.*, *34*(8), 2923–2939. doi: 10.1175/JCLI-D-20-0166.1
- Jonville, T., Borne, M., Flamant, C., Cuesta, J., Bock, O., Bosser, P., ... Knippertz, P. (2025, September). Impact of convectively coupled tropical waves on the composition, vertical structure of the atmosphere, and tropical cyclogenesis in the region of Cabo Verde in September 2021 during the CADDIWA campaign. *Atmos. Chem. Phys.*, *25*(17), 9765–9786. doi: 10.5194/acp-25-9765-2025
- Jonville, T., Cornillault, E., Lavaysse, C., Peyrillé, P., & Flamant, C. (2025, January). Distinguishing north and south African Easterly Waves with a spectral method: Implication for tropical cyclogenesis from mergers in the North Atlantic. *Quart J Royal Meteor Soc*, *151*(767), e4909. doi: 10.1002/qj.4909
- Karnauskas, K. B., Zhang, L., & Emanuel, K. A. (2021, April). The Feedback of Cold Wakes on Tropical Cyclones. *Geophysical Research Letters*, *48*(7), e2020GL091676. doi: 10.1029/2020GL091676
- Keenlyside, N. S., & Latif, M. (2007, January). Understanding Equatorial Atlantic Interannual Variability. *J. Clim.*, *20*(1), 131–142. doi: 10.1175/JCLI3992.1
- Keil, P., Schmidt, H., Stevens, B., & Bao, J. (2021, September). Variations of Tropical Lapse Rates in Climate Models and their Implications for Upper Tropospheric Warming. *J. Clim.*, 1–50. doi: 10.1175/JCLI-D-21-0196.1
- Kim, D., Lee, S.-K., Lopez, H., Foltz, G. R., Wen, C., West, R., & Dunion, J. (2023, June). Increase in Cape Verde hurricanes during Atlantic Niño. *Nat Commun*, *14*(1), 3704. doi: 10.1038/s41467-023-39467-5
- Klotzbach, P. J. (2010, January). On the Madden–Julian Oscillation–Atlantic Hurricane Relationship. *J. Clim.*, *23*(2), 282–293. doi: 10.1175/2009JCLI2978.1

- Klotzbach, P. J. (2011, February). El Niño–Southern Oscillation’s Impact on Atlantic Basin Hurricanes and U.S. Landfalls. *J. Clim.*, *24*(4), 1252–1263. doi: 10.1175/2010JCLI3799.1
- Klotzbach, P. J., Bercos-Hickey, E., Wood, K. M., Schreck, C. J., Bell, M. M., Blake, E. S., . . . Uehling, J. (2025, October). The Remarkable 2024 North Atlantic Mid-Season Hurricane Lull. *Geophysical Research Letters*, *52*(19), e2025GL116714. doi: 10.1029/2025GL116714
- Klotzbach, P. J., & Oliver, E. C. J. (2015, May). Variations in global tropical cyclone activity and the Madden-Julian Oscillation since the midtwentieth century. *Geophysical Research Letters*, *42*(10), 4199–4207. doi: 10.1002/2015GL063966
- Knaff, J. A. (1997, April). Implications of Summertime Sea Level Pressure Anomalies in the Tropical Atlantic Region. *J. Climate*, *10*(4), 789–804. doi: 10.1175/1520-0442(1997)010<0789:IOSSLP>2.0.CO;2
- Knutson, T., Camargo, S. J., Chan, J. C. L., Emanuel, K., Ho, C.-H., Kossin, J., . . . Wu, L. (2020, March). Tropical Cyclones and Climate Change Assessment: Part II: Projected Response to Anthropogenic Warming. *Bull. Am. Meteorol. Soc.*, *101*(3), E303–E322. doi: 10.1175/BAMS-D-18-0194.1
- Kossin, J. P., & Vimont, D. J. (2007, November). A More General Framework for Understanding Atlantic Hurricane Variability and Trends. *Bull. Amer. Meteor. Soc.*, *88*(11), 1767–1782. doi: 10.1175/BAMS-88-11-1767
- Landsea, C. W., & Franklin, J. L. (2013, October). Atlantic Hurricane Database Uncertainty and Presentation of a New Database Format. *Mon. Weather Rev.*, *141*(10), 3576–3592. doi: 10.1175/MWR-D-12-00254.1
- Lawton, Q. A., & Majumdar, S. J. (2023, July). Convectively Coupled Kelvin Waves and Tropical Cyclogenesis: Connections through Convection and Moisture. *Mon. Weather Rev.*, *151*(7), 1647–1666. doi: 10.1175/MWR-D-23-0005.1
- Lawton, Q. A., Majumdar, S. J., Dotterer, K., Thorncroft, C., & Schreck, C. J. (2022, August). The Influence of Convectively Coupled Kelvin Waves on African Easterly Waves in a Wave-Following Framework. *Mon. Weather Rev.*, *150*(8), 2055–2072. doi: 10.1175/MWR-D-21-0321.1
- Lu, M., Deng, K., Yang, S., Zhou, G., & Tan, Y. (2017, October). Interannual and Interdecadal Variations of the Mid-Atlantic Trough and Associated American–Atlantic–Eurasian Climate Anomalies. *Atmosphere-Ocean*, *55*(4-5), 284–292. doi: 10.1080/07055900.2017.1369931
- Maloney, E. D., & Hartmann, D. L. (2000, March). Modulation of Hurricane Activity in the Gulf of Mexico by the Madden-Julian Oscillation. *Science*, *287*(5460), 2002–2004. doi: 10.1126/science.287.5460.2002
- McTaggart-Cowan, R., Davies, E. L., Fairman, J. G., Galarneau, T. J., & Schultz, D. M. (2015, November). Revisiting the 26.5°C Sea Surface Temperature Threshold for Tropical Cyclone Development. *Bull. Am. Meteorol. Soc.*, *96*(11), 1929–1943. doi: 10.1175/BAMS-D-13-00254.1
- Ndiaye, O., Goddard, L., & Ward, M. N. (2009, July). Using regional wind fields to improve general circulation model forecasts of July–September Sahel rainfall. *Intl Journal of Climatology*, *29*(9), 1262–1275. doi: 10.1002/joc.1767
- NHC. (2025, October). *Tropical Storm Melissa discussion number 10*. <https://www.nhc.noaa.gov/archive/2025/al13/al132025.discus.010.shtml>. (Accessed 28th November 2025.)
- NHC. (2026). *Tropical Cyclone Reports*. <https://www.nhc.noaa.gov/data/tcr/index.php>. (Accessed 11th February 2026.)
- NOAA. (2025, January). *Noaa enso diagnostic discussion*. [https://www.cpc.ncep.noaa.gov/products/analysis\\_monitoring/enso\\_advisory/](https://www.cpc.ncep.noaa.gov/products/analysis_monitoring/enso_advisory/). (Accessed 28th November 2025.)
- NOAA. (2026). *Destructive 2018 Atlantic hurricane season draws to an end*. <https://www.noaa.gov/media-release/destructive-2018-atlantic>

- hurricane-season-draws-to-end. (Accessed 17 February 2026.)
- Okumura, Y., & Xie, S.-P. (2004, September). Interaction of the Atlantic Equatorial Cold Tongue and the African Monsoon\*. *J. Climate*, *17*(18), 3589–3602. doi: 10.1175/1520-0442(2004)017<3589:IOTAEC>2.0.CO;2
- Physical Sciences Laboratory, N. (2026). *Atlantic Meridional Mode Index*. <https://psl.noaa.gov/data/timeseries/month/DS/AMM/>. (Accessed 13 February 2026.)
- Pu, B., & Cook, K. H. (2012, April). Role of the West African Westerly Jet in Sahel Rainfall Variations. *J. Clim.*, *25*(8), 2880–2896. doi: 10.1175/JCLI-D-11-00394.1
- Rajasree, V., Cao, X., Ramsay, H., Núñez Ocasio, K. M., Kilroy, G., Alvey, G. R., ... Yu, H. (2023, September). Tropical cyclogenesis: Controlling factors and physical mechanisms. *Tropical Cyclone Research and Review*, *12*(3), 165–181. doi: 10.1016/j.tcr.2023.09.004
- Rios-Berrios, R., Finocchio, P. M., Alland, J. J., Chen, X., Fischer, M. S., Stevenson, S. N., & Tao, D. (2024, April). A Review of the Interactions between Tropical Cyclones and Environmental Vertical Wind Shear. *J. Atmospheric Sci.*, *81*(4), 713–741. doi: 10.1175/JAS-D-23-0022.1
- Rios-Berrios, R., Tang, B. H., Davis, C. A., & Martinez, J. (2024, October). Modulation of Tropical Cyclogenesis by Convectively Coupled Kelvin Waves. *Mon. Weather Rev.*, *152*(10), 2309–2322. doi: 10.1175/MWR-D-24-0052.1
- Russell, J. O., Ayyer, A., White, J. D., & Hannah, W. (2017, January). Revisiting the connection between African Easterly Waves and Atlantic tropical cyclogenesis. *Geophysical Research Letters*, *44*(1), 587–595. doi: 10.1002/2016GL071236
- Sampson, C. R., & Schrader, A. J. (2000, June). The Automated Tropical Cyclone Forecasting System (Version 3.2). *Bull. Amer. Meteor. Soc.*, *81*(6), 1231–1240. doi: 10.1175/1520-0477(2000)081<1231:TATCFS>2.3.CO;2
- Schneider, D. P., Deser, C., Fasullo, J., & Trenberth, K. E. (2013, March). Climate Data Guide Spurs Discovery and Understanding. *EoS Transactions*, *94*(13), 121–122. doi: 10.1002/2013EO130001
- Schreck, C. J. (2016, November). Convectively Coupled Kelvin Waves and Tropical Cyclogenesis in a Semi-Lagrangian Framework. *Mon. Weather Rev.*, *144*(11), 4131–4139. doi: 10.1175/MWR-D-16-0237.1
- Schreck, C. J., Molinari, J., & Ayyer, A. (2012, March). A Global View of Equatorial Waves and Tropical Cyclogenesis. *Mon. Weather Rev.*, *140*(3), 774–788. doi: 10.1175/MWR-D-11-00110.1
- Sears, J., & Velden, C. S. (2014). Investigating the Role of the Upper-Levels in Tropical Cyclone Genesis. *Trop. Cyclone Res. Rev.*, *3*(2), 91–110.
- Thorncroft, C., & Hodges, K. (2001, March). African Easterly Wave Variability and Its Relationship to Atlantic Tropical Cyclone Activity. *J. Climate*, *14*(6), 1166–1179. doi: 10.1175/1520-0442(2001)014<1166:AEWVAI>2.0.CO;2
- Trenberth, K. E., & Shea, D. J. (2006, June). Atlantic hurricanes and natural variability in 2005. *Geophysical Research Letters*, *33*(12), 2006GL026894. doi: 10.1029/2006GL026894
- UCAR. (2025, November). *Record-breaking winds confirmed for Hurricane Melissa*. <https://news.ucar.edu/133047/record-breaking-winds-confirmed-hurricane-melissa>. (Accessed 28th November 2025.)
- Vellinga, M., Arribas, A., & Graham, R. (2013, June). Seasonal forecasts for regional onset of the West African monsoon. *Clim Dyn*, *40*(11-12), 3047–3070. doi: 10.1007/s00382-012-1520-z
- Ventrice, M. J., Thorncroft, C. D., & Janiga, M. A. (2012, April). Atlantic Tropical Cyclogenesis: A Three-Way Interaction between an African Easterly Wave, Diurnally Varying Convection, and a Convectively Coupled Atmospheric Kelvin Wave. *Mon. Wea. Rev.*, *140*(4), 1108–1124. doi: 10.1175/MWR-D-11-00122.1
- Ventrice, M. J., Thorncroft, C. D., & Schreck, C. J. (2012, July). Impacts of Convectively Coupled Kelvin Waves on Environmental Conditions for At-

- lantic Tropical Cyclogenesis. *Mon. Weather Rev.*, *140*(7), 2198–2214. doi: 10.1175/MWR-D-11-00305.1
- Vimont, D. J., & Kossin, J. P. (2007, April). The Atlantic Meridional Mode and hurricane activity. *Geophysical Research Letters*, *34*(7), 2007GL029683. doi: 10.1029/2007GL029683
- Wang, Y., Satoh, M., Zhan, R., Zhao, J., & Xie, S.-P. (2025, October). Tropical Sea Surface Warming Patterns and Tropical Cyclone Activity: A Review. *Adv. Atmos. Sci.*, *42*(10), 1996–2017. doi: 10.1007/s00376-025-5114-1
- Wheeler, M. C., & Hendon, H. H. (2004, August). An All-Season Real-Time Multivariate MJO Index: Development of an Index for Monitoring and Prediction. *Mon. Wea. Rev.*, *132*(8), 1917–1932. doi: 10.1175/1520-0493(2004)132<1917:AARMMI>2.0.CO;2
- Wilks, D. S. (2006). *Statistical methods in the atmospheric sciences* (2nd ed ed.) (No. volume 91). Amsterdam Paris: Elsevier.
- Williams, A. I. L., Jeevanjee, N., & Bloch-Johnson, J. (2023, March). Circus Tents, Convective Thresholds, and the Non-Linear Climate Response to Tropical SSTs. *Geophysical Research Letters*, *50*(6), e2022GL101499. doi: 10.1029/2022GL101499
- Xia, F., Zuo, J., Sun, C., & Liu, A. (2023, February). The Atlantic Meridional Mode and Associated Wind–SST Relationship in the CMIP6 Models. *Atmosphere*, *14*(2), 359. doi: 10.3390/atmos14020359
- Zhang, G., & Cook, K. H. (2014, September). West African monsoon demise: Climatology, interannual variations, and relationship to seasonal rainfall. *JGR Atmospheres*, *119*(17). doi: 10.1002/2014JD022043